axioms

MDPI

*Article*

# Adaptive Enhancement for Coal-Rock Cutting Sound Based on Parameter Self-Tuning Bistable Stochastic Resonance Model

**Jie Xu [1], Jing Xu [1,2,*], Chaofan Ren [1], Yanxin Liu [1] and Ning Sun [1]**

[1] School of Mechanical Engineering, Jiangsu University of Science and Technology, No. 2 Mengxi Road, Zhenjiang 212114, China; xujie9js@163.com (J.X.); rcf666888@163.com (C.R.); lyanxin1998@163.com (Y.L.); 15262132649@163.com (N.S.)

[2] Marine Equipment and Technology Institute, Jiangsu University of Science and Technology, No. 2 Mengxi Road, Zhenjiang 212008, China

* Correspondence: xujing@just.edu.cn; Tel.: +86-511-8889-2131; Fax: +86-511-8889-2131

**Abstract:** The traditional bistable stochastic resonance model has always had the drawback of being difficult when choosing accurate system parameters when a weak signal is enhanced. This paper proposes a parameter self-tuning adaptive optimization method based on the bat optimization algorithm to address this issue. The cubic mapping strategy of chaos optimization is introduced in the initial process of the individual position of the bat algorithm. Chaos is characterized by randomness, sensitivity, fractal dimension, and universality. The initial problem of the algorithm falling into local extremums is overcome. The global search capability of the basic bat optimization algorithm has been improved. The improved bat optimization algorithm's objective function is the signal-to-noise ratio (SNR) of the target weak signal output by the bistable stochastic resonance model. An adaptive signal enhancement algorithm based on the improved bat optimization algorithm and bistable stochastic resonance (IBA-BSR) model is constructed to increase the proportion of weak signals in the mixed signal. Simulation signals are created to validate the proposed algorithm's feasibility. The engineering application effect of this algorithm is further demonstrated by enhancing the sound signal of coal and rock cutting by a shearer in a coal face. Engineering test results demonstrate that this algorithm can significantly increase the SNR of coal and rock cutting sound signals by 42.4537 dB, and the effect is remarkable.

**Keywords:** bistable stochastic resonance; bat optimization algorithm; chaotic cubic mapping; weak signal enhancement; coal-rock cutting sound signal

**MSC:** 49-XX



**Citation:** Xu, J.; Xu, J.; Ren, C.; Liu, Y.; Sun, N. Adaptive Enhancement for Coal-Rock Cutting Sound Based on Parameter Self-Tuning Bistable Stochastic Resonance Model. *Axioms* **2022**, *11*, 246. https://doi.org/10.3390/axioms11060246

Academic Editors: Eric Campos-Cantón, Ernesto Zambrano-Serrano, Guillermo Huerta Cuellar and Esteban Tlelo-Cuautle

Received: 6 April 2022
Accepted: 7 May 2022
Published: 25 May 2022



## 1. Introduction

With the rapid development of modern industry, electromechanical equipment is developing in a large-scale and complicated direction. It is of great significance to improve the intelligence level of machinery to study the method of condition monitoring, diagnosis, and realize the state identification of mechanical equipment. The vibration, sound, pressure, and other signals generated by the coal mining shearer's critical components during operation contain a wealth of useful information that can be used to characterize the equipment's operating and load states [1,2]. Vibration and pressure signals used in coal-rock cutting share several disadvantages, including contact measurement, limited detection positions, and difficulty maintaining detectors in certain severe situations. As a result, vibration and pressure measurements become ineffective, if not impossible, in these situations. On the other hand, the cutting sound signal produced when the cutting unit collides with coal or rock can be used as a critical standard for state recognition and fault diagnosis, as it has the advantages of non-contact measurement, compact structure, low power consumption, is easy to collect, and does not affect the machine [3]. However,

the sound signal collected directly from the industrial area is always contaminated by a large amount of noise and irrelevant signals. In the worst-case scenario, the target signal may become completely "submerged" in the mixed signal. Finally, it results in a low SNR for the target signal, impairing subsequent feature extraction and recognition effects. Thus, increasing the SNR of weak target signals in the presence of high background noise is critical for achieving state identification and intelligent control of electromechanical equipment operating in harsh environments [4,5]. Preliminary research shows that stochastic resonance has certain advantages in improving the SNR ratio of the weak signal under strong background noise [6].

Benzi et al. [7] are scholars who proposed stochastic resonance in 1981 while studying the interaction of the climate system's internal nonlinearity and external orbital forcing. Benzi makes periodic changes in the output of the periodic driving force and noise-driven signal via the nonlinear system to transfer some of the noise's energy to the signal to be measured, thereby enhancing the target's weak signal [8]. Stochastic resonance is widely used to detect faults in rotating machinery, detect the looseness state of small components, and detect abnormalities in building structures [9,10]. Bistable systems are a type of nonlinear system that is frequently used to study classical stochastic resonances. There are two steady points and one unsteady point in a bistable system. The vertical distance between the steady point and the unsteady point is referred to as the potential well height [11]. The results indicate that the potential well height significantly affects the bistable stochastic resonance model's effect. When the potential well height is too small, the effect of system resonance is not obvious, and when it is too large, system resonance cannot be generated [12]. In [13], a new advancing coupled multi-stable stochastic resonance method, namely CMSR, was proposed, which uses two first-order multi-steady state stochastic resonance systems to detect motor bearing faults. Combined with numerical simulation and sub-sampling techniques, the system parameters were optimized adaptively. [14] proposed a method for detecting multi-frequency signals based on frequency exchange and rescaling stochastic resonance (FERSR). Filter technology and single sideband (SSB) modulation were combined to achieve frequency exchange. In [15], a method for detecting faint signals in the presence of strong noise in sensors was proposed using stochastic resonance (SR). The power spectrum was used to evaluate the system. The SR phenomenon and fast Fourier transform (FFT) spectrum analysis were combined to detect the weak signal in mixed noise. In [16], Shan Wang et al. proposed an adaptive unsaturated stochastic resonance method, using maximum cross-correlation kurtosis as a signal detection index. Considering the random pulse of mechanical noise and the limitations of traditional measurement indexes requires knowing the characteristic frequency in advance to identify mechanical fault pulse signals. The method combines the characteristics of the correlation number to indicate the periodic fault transients and combines the characteristics of the spectrum kurtosis to locate these transients in the frequency domain.

The above research explored some adaptive methods of stochastic resonance system parameters and achieved certain results. In recent years, with the development of artificial intelligence, some scholars have used heuristic swarm optimization algorithms to optimize the parameters of stochastic resonance systems [17]. In [18], a novel adaptive multi-parameter unsaturation bistable stochastic resonance (AMUBSR) system based on piecewise linearization of potential function was proposed. The system parameters were optimized by beetle antenna search (BAS), with the output SNR as the objective function. Independent adjustments of barrier height, potential distance and opening size were achieved. Heng Wang et al. [19] proposed an early fault diagnosis method for rolling bearing based on noise-assisted signal feature enhancement and stochastic resonance. A particle swarm optimization algorithm was used to optimize the parameters of the system to achieve the best match between the system, the input signal, and the noise, so as to improve the stochastic resonance effect.

Bat algorithm [20] was a novel meta-heuristic algorithm developed in 2010 by Professor Yang, a famous British scholar, who was inspired by the echo characteristics of bats during

his research on particle swarm optimization, firefly optimization, and simulated annealing optimization. Natural bats expand their search area during hunting by varying the intensity of ultrasonic pulses and localize prey by varying the emission frequency. The bat algorithm determines the global optimal value by simulating bat foraging behavior. Compared with other algorithms, the bat algorithm has the advantages of a simple model, fewer parameters, and fast convergence [21,22]. The bat algorithm has been widely applied in data classification [23], image segmentation [24], face recognition [25], etc. Bat algorithm has strong convergence and the ability to deal with multidimensional problems. However, the basic bat algorithm is easy to fall into the local optimum, which affects the optimization effect [26,27]. In order to avoid the bat algorithm falling into the local optimum, some improved methods were proposed. In [28], a new particle filter algorithm based on the bat algorithm was introduced. This method combines the bat algorithm and particle filter to improve the particle filter's accuracy while increasing particle diversity. Ref. [29] proposes an enhanced adaptive bat algorithm (EABA) for energy scheduling optimization in a microgrid system. In EABA, a mechanism for information sharing and interaction between bats is added to improve search performance. Yuan et al. proposed path planning for mobile robots based on an improved bat algorithm in 2021 [30]. They combined the bat algorithm and a dynamic window approach to meet global optimal and dynamic obstacle avoidance requirements in path planning for a mobile robot (DWA). Additionally, an undirected weighted graph is constructed using virtual points to provide the robot with a path switching strategy. The results indicate that this method can significantly reduce the length of the path. Tang et al. improved multi-robot path planning by incorporating a multi-group strategy and an adaptive inertial weight strategy. An improved bat algorithm was proposed for multi-robot target searching in unknown environments [31]. In addition to the above-improved strategies, Table 1 visually presents other strategies for improving bat algorithms. In recent years, many improvements have been made to bat algorithms, but few researchers have considered how to avoid falling into local optimality during algorithm initialization.

**Table 1.** Improved strategies for other bat algorithms.

| Algorithm Name | Time | Improvement Idea | The Optimization Effect | Application Field |
|---|---|---|---|---|
| hBBA [32] | 2020 | Analyze similarities between individuals and Detection of early convergence | The convergence of the algorithm is improved | Feature selection |
| MOBA [33] | 2021 | Mean square error and conjugate gradient method are combined | Improve global search capability | scheduling of resources |
| IBBA [34] | 2022 | Combining multi V-shaped transfer function and adaptive search space | Optimize the quality of understanding | Transmission network expansion planning |

According to previous studies, stochastic resonance has a good effect on weak signal enhancement under strong noise background. The system parameters of stochastic resonance have a very important effect on the effect of stochastic resonance. System parameters are correlated. It is always difficult to find a suitable set of system parameters in a search space. A biological algorithm has a great advantage in multidimensional problem analysis. In this paper, the bistable stochastic resonance model and the bat optimization algorithm are combined to optimize the parameters affecting the potential well height in the bistable stochastic resonance model and increase the SNR of the shearer's coal-rock cutting sound signal in the mixed signal. To overcome the parameter selection problem of the traditional bistable stochastic resonance system, the bat algorithm was introduced to perform global optimization. At the same time, to avoid the bat algorithm easily falling into a local extremum during initialization, the chaotic cubic mapping theory is used to evenly distribute the initial bat individuals' positions. The global optimization ability of the bat algorithm was enhanced and the convergence accuracy was improved. This algorithm analyzes the shearer's simulation signal as well as the cutting coal and rock signal. Finally, the output

results demonstrate the feasibility and effectiveness of the proposed IBA-BSR-based weak signal adaptive enhancement algorithm.

The next contents of this paper are organized as follows:

In Section 2, the principle of bistable stochastic resonance and bat algorithm was introduced in detail, and the signal-to-noise ratio was taken as the objective function.

In Section 3, the principle of the improved bat algorithm was analyzed in detail, and the improved bat algorithm was combined with the bistable stochastic resonance.

In Section 4, the superiority of the proposed algorithm was proved by processing multiple groups of simulation signals.

In Section 5, each algorithm was used to process coal-rock cutting sound signal, and the practicability of the proposed algorithm was verified.

In Section 6, the author summarized the article and put forward the next work plan.

## 2. Algorithm Overview

### *2.1. Bistable Stochastic Resonance Model*

The conventional bistable system exhibits the characteristics of a double potential well, which serves as the foundation for studying the stochastic resonance model. The following is the specific expression:

$$U(x) = -\frac{a}{2}x^2 + \frac{b}{4}x^4 \tag{1}$$

where $U(x)$ is also called potential function, $a$ and $b$ are system parameters, and both are positive numbers. The potential function has two steady-state points $x_{\pm} = \pm\sqrt{a/b}$ and one unsteady state point $x_{un} = 0$. The width between the two steady-state points is $\Delta x = 2\sqrt{a/b}$, where the vertical distance from the steady-state point to the non-steady-state point is called the potential well height $\Delta U = a^2/4b^2$.

By adjusting the system parameters, $a$ and $b$, the potential function's potential well width and height can be varied, resulting in the generation of potential functions of various shapes, as illustrated in Figure 1. The potential function's potential well width and height are proportional to the change in $a$ and inversely proportional to the change in $b$. The system parameters $a$ and $b$ have opposing effects on the potential function, respectively, restricting and balancing it. As a result, simultaneous adjustment of the values of $a$ and $b$ is required to obtain an appropriate potential function. By adjusting the potential field force of the particles in the bistable system, the effect of stochastic resonance can be altered.

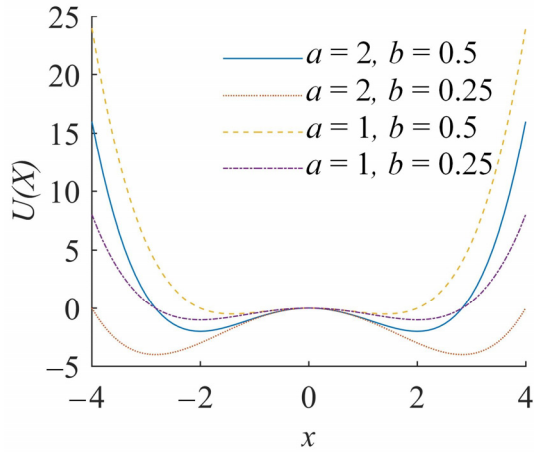


**Figure 1.** The potential function with different parameters.

The classical bistable stochastic resonance system modifies the traditional bistable system that incorporates an input signal. The Langevin equation that corresponds is as follows:

$$\frac{dx}{dt} = -\dot{U}(x) + S(t) + N(t) \tag{2}$$

where $x$ represents particle track, $\dot{U}(x) = -ax + bx^3$, $S(t) = A\cos(2\pi ft)$ represents a weak signal of the actual input, $A$ is the signal amplitude, and $f$ is the signal frequency. $N(t) = \sqrt{2D}\xi(t)$ is additive white Gaussian noise. Where the noise intensity is $D$, the mean is zero, and the variance is 1. The specific mathematical properties are as follows:

$$\begin{aligned} &E\langle N(t)\rangle = 0 \\ &E\langle N(t)N(t+\tau)\rangle = 2D\delta(\tau) \end{aligned} \tag{3}$$

The bistable stochastic resonance system needs to meet the adiabatic approximation theory [35], which requires the solution under the condition of small frequency, but the actual signal is usually inconsistent. Leng Yonggang et al. [36] proposed the method of secondary sampling to solve this limitation. Given the compression ratio $M$, set the original signal frequency to be $f$, the compression signal frequency is $f'$; The original sampling frequency is $fs$ and the compressed sampling frequency is $fs'$. The signal frequency is compressed by $f/f' = fs/fs' = M$, solved, and then reduced in the same proportion.

The Langevin equation is transformed into a difference equation for numerical solution in this paper using the fourth-order Runge–Kutta algorithm [37]. The discrete bistable stochastic resonance system is incorporated into the fourth-order Runge–Kutta algorithm via the following specific formula:

$$\begin{aligned} k_1 &= h\left[ax_n - bx_n^3 + d_n\right] \\ k_2 &= h\left[a(x_n + \tfrac{k_1}{2}) - b(x_n + \tfrac{k_1}{2})^3 + d_n\right] \\ k_3 &= h\left[a(x_n + \tfrac{k_2}{2}) - b(x_n + \tfrac{k_2}{2})^3 + d_{n+1}\right] \\ k_4 &= h\left[a(x_n + k_3) - b(x_n + k_3)^3 + d_{n+1}\right] \end{aligned} \tag{4}$$

where $d_n = S(n) + N(n)$ is the input signal of the system, $S(n)$ is the weak signal, $N(n)$ is the input noise signal, and $h = 1/fs$ is the step size of calculation.

The output SNR is used to describe the output effect of a classical bistable system. The output SNR is expressed as follows:

$$f(x) = SNR = 10\lg\frac{p_0}{(\sum_{i=0}^{n} p_i - p_0)/n} \tag{5}$$

where $p_0$ is the power spectrum at the weak characteristic frequency, $p_i$ is the power spectrum corresponding to the characteristic frequency at $i$, and $(\sum_{i=0}^{n} p_i - p_0)/n$ is the average power spectrum of background noise. The target signal is input into the bistable system and Fourier transform is performed to obtain the power spectrum of the output signal. The obtained power spectrum is substituted into Formula (5) to obtain the SNR of the output signal. As can be seen from the above analysis process, when the sampling frequency and sampling step are constant, the different values of $a$ and $b$ will directly affect the system's output signal-to-noise ratio, thus determining the enhancement effect of the bistable stochastic resonance system on the target signal.

### *2.2. Bat Algorithm*

Yang et al. proposed the bat algorithm as a novel intelligent swarm optimization method in 2010 [20]. BA is a novel algorithm for population evolution. Each bat's location indicated a potential solution to the problem.

It is assumed that bats are hunting in $D$-dimensional space, and they constantly change their pulse frequency and flight speed during the flight to update their position to achieve the optimal hunting effect [38]. Pulse frequency, flight speed, and position update rules are as follows:

$$f_i = f_{\min} + (f_{\max} - f_{\min}) \times \beta \tag{6}$$

$$v_i^t = v_i^{t-1} + (x_i^t - x_*) \times f_i \tag{7}$$

$$x_i^t = x_i^{t-1} + v_i^t \tag{8}$$

where $\beta$ is a random number in the range 0 to 1, $f_i$ is the pulse frequency, the adjustment interval is from $f_{\min}$ to $f_{\max}$, $x_*$ is the current optimal position of the bat, $x_i^t$, $v_i^t$ represent, respectively, the position and velocity searched by the $i$-th bat at time $t$.

When an optimal position is determined, a random number between (0, 1) is generated and compared to the current pulse rate, disrupting and updating the current search position. The following rules apply to updates:

$$x_{new} = x_{old} + \varepsilon A^t \tag{9}$$

where $\varepsilon$ is a random number between $-1$ and 1 and $A^t$ is the average loudness of this generation of bats at time $t$.

Bats will emit a high loudness and a pulse rate during the initial search process and will constantly update their loudness and pulse rate in response to the hunting target to catch prey faster. As the bat approaches its prey, it lowers its pitch and increases its pulse rate to focus its search and pinpoint its prey. The following are the rules for updating the loudness and pulse rate:

$$A_i^{t+1} = \alpha \times A_i^t \tag{10}$$

$$r_i^{t+1} = r_i^0[1 - \exp(-\gamma \times t)] \tag{11}$$

where $\alpha$ belongs to (0, 1), is the attenuation coefficient of bat emission loudness; $A_i^t$ represents the loudness of the $i$-th bat at time $t$; A positive $\gamma$ is the enhancement coefficient of the pulse rate emitted by bats; $r_i^0$ represents the initial pulse rate of the $i$-th bat; $r_i^{t+1}$ represents the pulse rate of the $i$-th bat at time $t + 1$. $\alpha$ and $\gamma$ are generally obtained by experiment, usually $\alpha = \gamma = 0.9$.

The traditional bat algorithm flow is as follows:

Step 1: Initialize bat populations $n$, population size $m$, iteration times $N$, objective function $f(x)$, bat position $x_i$ ($i$ = 1, 2, . . . , $m$) and velocity $v_i$, the pulse frequency $f_i$, acoustic loudness $A_i$ and the pulse rate $r_i$.

Step 2: Initializes the position of each individual bat in the search space. The comparison produces an initial optimal fitness value.

Step 3: The frequency, velocity, and position of individual bats were updated according to Formulas (6)–(8).

Step 4: Random disturbance. If $rand > r_i$, a local solution is obtained by perturbing through Formula (9); otherwise, the bat position is updated according to Formula (8).

Step 5: The current best solution is generated.

Step 6: Update acoustic loudness and pulse rate. If $rand < A_i$ and fitness value are better than the new solution in Step 5, this position is accepted, the pulse loudness $A_i$ of the bat $i$ is reduced, and the pulse rate $r_i$ of the bat $i$ is increased according to Formulas (10) and (11); otherwise, use the previous position.

Step 7: Global optimal evaluation. The fitness of all individuals in the current population was calculated to obtain the global optimal fitness and the corresponding bat position.

Step 8: Iteration terminated. If the current iteration number reaches the maximum, stop the iteration; otherwise, repeat Steps 3~7.

## 3. Weak Signal Adaptive Enhancement Algorithm Based on the IBA-BSR Model

### *3.1. Improved Bat Optimization Algorithm*

During the initialization of the bat algorithm, the bat's initial position is determined randomly, which does not ensure a uniform distribution of the search space [39]. As a result, the algorithm initially becomes stuck in some local extremes and is unable to escape. Simultaneously, it will attract a large number of groups to gather, reducing the population's ability to optimize globally.

This paper solves this problem by optimizing the initialization of the bat position using chaos optimization theory. Chaos has randomness, universality, and fractal dimensions, which equalizes the distribution of the bat population in search spaces and enhances the global search capability of the bat algorithm.

This paper uses chaotic optimization to initialize bat positions via cubic mapping [40]. First, cubic mapping can be used to generate a series of uniformly distributed random numbers in the solution space. Then, bats can be distributed randomly and uniformly within the corresponding space using certain rules. The following is the formula:

$$y_{i+1,d} = 4y_{i,d}^3 - 3y_{i,d} \tag{12}$$

$$x_{i,d} = L + (1 + y_{i,d}) \cdot (U - L)/2 \tag{13}$$

where $y_{i,d}$ represents the $d$-th component factor of the $i$-th bat in D-dimensional space, $U$ and $L$ represent the upper and lower limits of the search space, respectively. $x_{i,d}$ represents the initial position corresponding to the $d$ component of the $i$ bat in the $D$-dimensional space under the action of corresponding factors.

The pseudocode of the improved bat algorithm is shown in Algorithm 1 [20]:

**Algorithm 1** Improved Bat Algorithm

Initialize $m, f_i, \alpha, \gamma, N, x_i, ri, Ai$ and the objective function $f(\cdot)$.
Initialize the position and velocity of each bat according to Equations (12) and (13).
Find the best position.
while ($n < N$)
Update the bat frequency, speed and position according to the Equations (6)–(8).
    if (rand (0, 1) > $ri$)
        Generate a local optimal solution according to the Equation (9).
    end if
    Evaluate the fitness of all bats and search the best one $x^*$.
    if (rand (0, 1) < $Ai$ & $f(x_i) < f(x^*)$)
        Accept the previous optimal solution.
        Update the loudness and emission frequency according to the Equations (10) and (11).
    end if
Search the current best bat.
$n = n + 1$.
end while
Postprocess the results and visualization.

### *3.2. Weak Signal Enhancement Algorithm Flow Based on an IBA-BSR Model*

Variation of the system parameters $a$ and $b$ in the bistable stochastic resonance system affects the horizontal spacing and height of the potential well function, which in turn affects the effect of stochastic resonance. This paper aims to present a weak signal enhancement algorithm based on an improved bat optimization algorithm and a bistable stochastic resonance model for optimizing the system parameters $a$ and $b$ to maximize the target signal SNR. The algorithm's specific procedure is as follows:

Step 1: Initialize the sampling frequency of the input signal $fs$, signal compression ratio $M$, number of bat populations $n$, population size $m$, iteration times $N$, output SNR of the signal as objective function $f(x)$, bat position $x_i$ ($i$ = 1, 2, . . . , $m$) and velocity $vi$, the pulse frequency $f_i$, acoustic loudness $A_i$, and the pulse rate $r_i$. The bat positions are made uniformly distributed by cubic mapping, and the positions are initialized according to Formulas (12) and (13).

Step 2: To obtain the corresponding output signal, the bat position is passed to the fourth-order Runge–Kutta algorithm as a system parameter. The maximum output SNR and corresponding bat position are determined by comparing a series of output SNR obtained using Formula (5).

Step 3: The frequency, velocity, and position of individual bats were updated according to Formulas (6)–(8).

Step 4: A random number *rand* in the range (0, 1) is generated and compared with the pulse rate $r_i$ for each parameter. If $rand > r_i$, a local solution is obtained by perturbing through Formula (9); otherwise, the bat position is updated according to Formula (8).

Step 5: According to the process of Step 2, the corresponding output SNR is obtained by substituting the resulting bat position.

Step 6: Then, generate a random number *rand* in the range of (0, 1). If $rand < A_i$ and the output SNR is better than the new solution in Step 5, this position is accepted, the pulse loudness $A_i$ of the bat $i$ is reduced, and the pulse rate $r_i$ of the bat $i$ is increased according to Formulas (10) and (11); otherwise, use the previous position.

Step 7: According to Step 2, all positions in the current population are substituted, and the current optimal position X* is determined through comparison. The maximum output SNR is then compared to the maximum output SNR from the previous iteration to update the global maximum output SNR and optimal location.

Step 8: If the current iteration count reaches the maximum or the error value satisfies the specified precision threshold, the iteration process is terminated. Otherwise, steps 3 through 7 are repeated. The algorithm's flow diagram is shown in Figure 2.

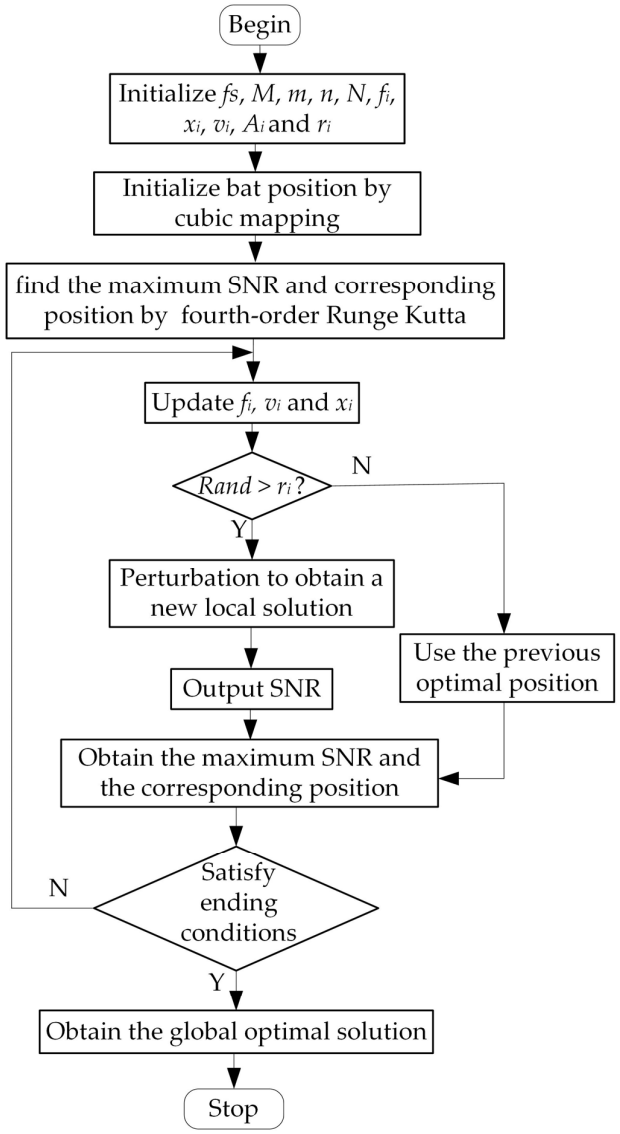


**Figure 2.** Algorithm flow chart.

## 4. Simulation and Comparative Analysis

### *4.1. Simulation Signal Construction and Evaluation Methods*

In this paper, simulation signals were used to verify the effectiveness of the proposed weak signal enhancement algorithm based on the IBA-BSR model. The original signal $s = A\sin(2 \times \pi \times f \times t)$ was constructed, where $A = 0.3$ dB represents the amplitude of the original signal and $f = 0.01$ Hz represents the frequency of the original signal. As shown in Figure 3, additive white Gaussian noise was added to the simulation signal, implying that the value was 0, the variance was 1, and the noise intensity was 0.6 dB, 0.8 dB, and 1 dB, respectively. The signal sampling frequency *fs* was set to 5 Hz, and the time and sampling steps were set to 0.2 s.

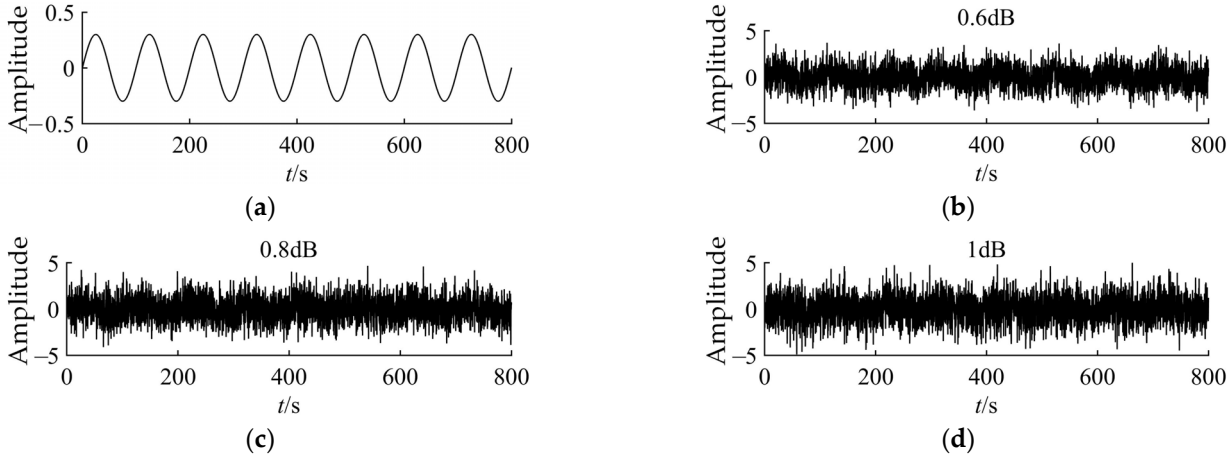


**Figure 3.** (**a**) Original signal; (**b**) Noise intensity is 0.6 dB; (**c**) Noise intensity is 0.8 dB; (**d**) Noise intensity is 1 dB.

### *4.2. Four Comparison Algorithm Parameter Settings*

In this paper, the enumeration method, particle swarm optimization algorithm proposed in reference [19], a traditional bat optimization algorithm, and an improved bat optimization algorithm were used to optimize the system parameters of a bistable stochastic resonance model, and the optimization effects of the various algorithms were compared. For the purpose of providing a detailed description, a noise intensity of 0.6 dB was used as an example.

(1) System parameters *a* and *b* were selected through the enumeration method, which was mainly divided into two parts [41]:

1.1 Fixing the parameter $a = 1$ and the output SNR as the objective function, parameter *b* was searched for in steps of 0.0001 in the range of (0, 10) to obtain $b = 1.2260$. Substitute the system parameters into the bistable stochastic resonance model to obtain the time–frequency diagram of the output signal, as shown in Figure 4.

1.2 The parameter $b = 1$ was fixed, the output SNR was the objective function, and the parameter a was sought in the range of (0, 10) in steps of 0.0001 to obtain $a = 1.1960$. The system parameters were substituted into the bistatic stochastic resonance model to obtain the output signal time–frequency diagram, as shown in Figure 5.

(2) According to analysis of the literature and to reduce the error caused by some parameter settings, the parameters of the particle swarm optimization algorithm were set as follows: The number of population was 2, the population size was $m = 100$, the range of system parameter *a* was (0, 10), the range of system parameter *b* was (0, 10), the self-learning factor was 1.4, the group learning factor was 1.4, the number of iterations was 500, the inertia weight was 0.8, and the velocity range of particles

was (−1, 1). The system parameters $a$ and $b$ calculated by the particle swarm optimization algorithm were 0.1034 and 0.4813, respectively. The system parameters were substituted into the bistable stochastic resonance model to obtain the time–frequency diagram of the output signal, as shown in Figure 6.

(3) The key parameters of the traditional bat algorithm were set as follows: the number of bats in the population $n$ = 2, the population size of bat $m$ = 100, the range of system parameter $a$ is (0, 10), the range of system parameter $b$ was (0, 10), the iteration number $N$ = 500, the pulse frequency range was (0, 1), the attenuation coefficient of loudness $\alpha$ = 0.9, and the enhancement coefficient of emission frequency $\gamma$ = 0.9. The system parameters $a$ and $b$ were calculated using the conventional bat optimization algorithm to be 0.0582 and 0.0122, respectively. The output signal's time–frequency diagram is shown in Figure 7, which was obtained by substituting the system parameters into the bistable stochastic resonance model.

(4) The initialization data of the improved bat optimization algorithm is consistent with that of the traditional bat optimization algorithm. The system parameters $a$ and $b$ calculated by the improved bat optimization algorithm were 0.0013 and 0.0037, respectively. The system parameters were substituted into the bistatic stochastic resonance model to obtain the output signal time–frequency diagram, as shown in Figure 8.

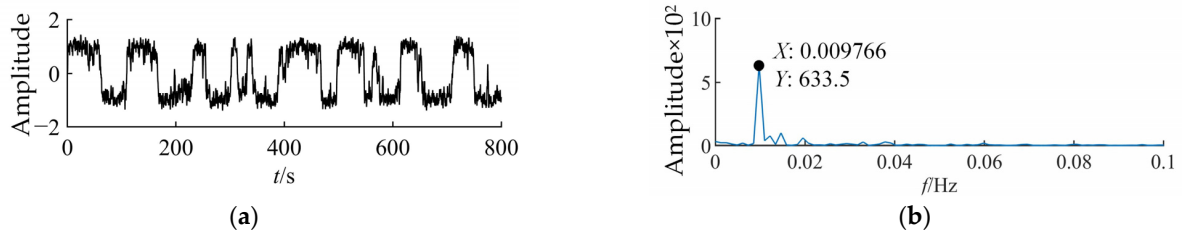


(**a**) (**b**)

**Figure 4.** (**a**) Output time domain waveform of stochastic resonance model based on enumeration method (fixed-parameter $a$); (**b**) Output spectrum of stochastic resonance model based on enumeration method (fixed-parameter $a$).

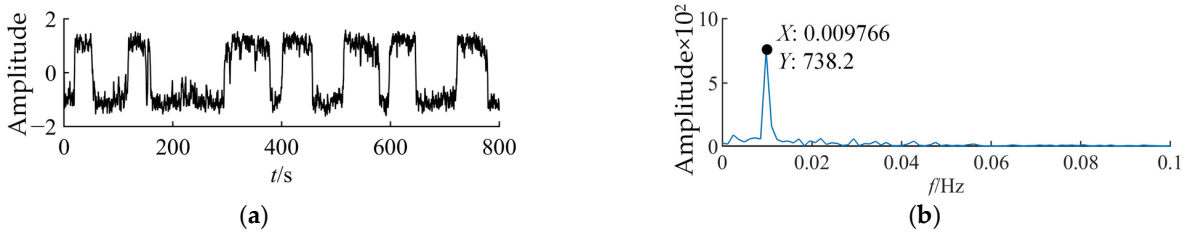


(**a**) (**b**)

**Figure 5.** (**a**) Output time domain waveform of stochastic resonance model based on enumeration method (fixed-parameter $b$); (**b**) Output spectrum of stochastic resonance model based on enumeration method (fixed-parameter $b$).

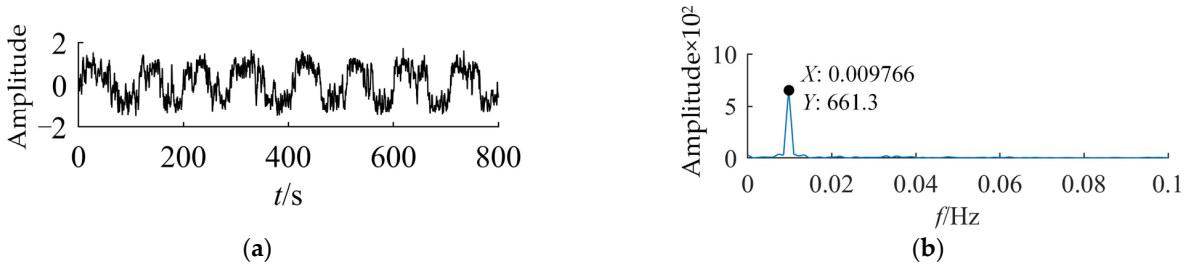


(**a**) (**b**)

**Figure 6.** (**a**) Output time domain waveform of stochastic resonance model based on particle swarm algorithm; (**b**) Output spectrum of stochastic resonance model based on particle swarm algorithm.

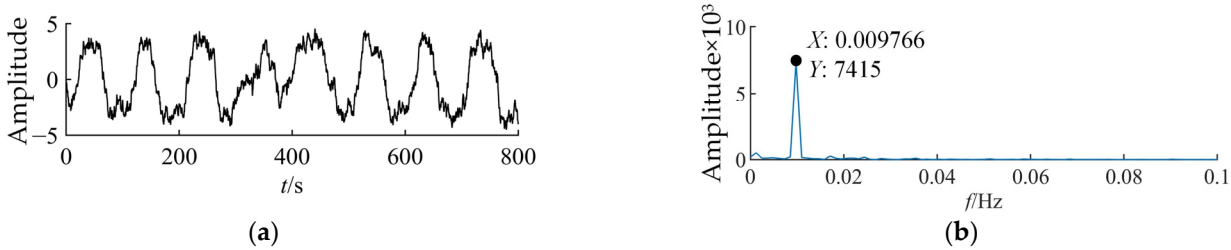


**Figure 7.** (**a**) Output time domain waveform of stochastic resonance model based on traditional bat optimization algorithm; (**b**) Output spectrum of stochastic resonance model based on the traditional bat optimization algorithm.

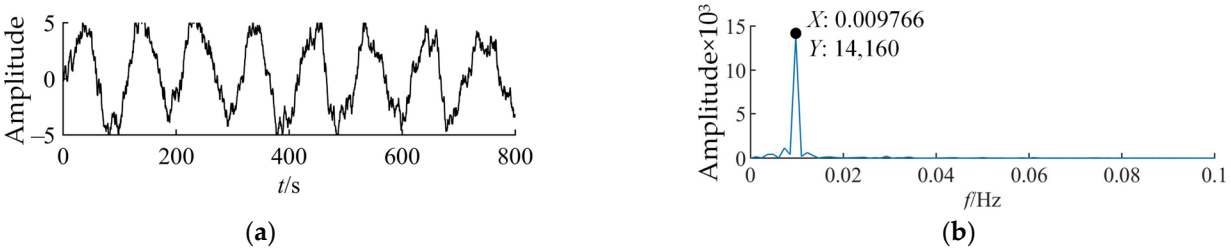


**Figure 8.** (**a**) Stochastic resonance model output time–domain waveform based on improved bat optimization algorithm; (**b**) Output spectrum of stochastic resonance model based on the improved bat optimization algorithm.

### *4.3. Data Conclusion Analysis*

As illustrated in Figures 4 and 5, the two enumeration methods have a comparable effect on optimizing system parameters. The amplitude was 633.5 dB and 738.2 dB at 0.009766 Hz, respectively, and the SNR was 31.0512 dB and 30.0243 dB.

Figure 6 showed the simulation effect of optimizing system parameters by the particle swarm optimization algorithm. It could be seen from the pattern that at the frequency of 0.009766 Hz, the corresponding amplitude was 661.3 dB, and the SNR ratio was 33.4295 dB.

The effect of the traditional bat optimization algorithm on optimizing system parameters is depicted in Figure 7. The amplitude was 7415 dB at 0.009766 Hz, and the SNR was 35.1677 dB. The results indicated that the enumeration method outperformed the traditional bat optimization algorithm.

Figure 8 illustrates the improved bat optimization algorithm's effect on system parameters optimization. At 0.009766 Hz, the amplitude is 14,160 dB and the signal-to-noise ratio is 39.1402 dB. The results indicated that the improved bat optimization algorithm outperformed the traditional algorithm.

Finally, the paper compares the enumeration method, the traditional bat optimization algorithm, the particle swarm optimization algorithm, and the improved bat optimization algorithm by adding different noise intensities to the simulation signal. In order to ensure the comparability of the results, the simulation parameters of each algorithm were set in accordance with the noise intensity of 0.6 dB. The SNR and calculation time of different algorithms in different noise intensities were shown in Tables 2 and 3.

**Table 2.** Corresponding SNR in the different algorithms.

| Input Noise Intensity/dB | Evaluation Indicators/dB | Fixed Parameter *a* | Fixed Parameter *b* | Particle Swarm Optimization | Traditional Bat Algorithm | Improved Bat Algorithm |
|---|---|---|---|---|---|---|
| 0.6 | SNR | 31.0512 | 30.0243 | 33.4295 | 35.1677 | **39.1402** |
| 0.8 | SNR | 29.2803 | 29.9231 | 32.7209 | 36.1041 | **39.2510** |
| 1.0 | SNR | 27.6950 | 27.9210 | 30.3497 | 34.9250 | **38.7179** |

**Table 3.** The calculation time of different algorithms.

| | Input Noise Intensity/dB | Fixed Parameter *a* | Fixed Parameter *b* | Particle Swarm Optimization | Traditional Bat Algorithm | Improved Bat Algorithm |
|---|---|---|---|---|---|---|
| Time/s | 0.6 | 188.571774 | 187.415857 | 93.799053 | **63.393899** | 93.934702 |
| | 0.8 | 188.079274 | 187.398719 | 94.220305 | **62.968921** | 93.908348 |
| | 1.0 | 188.929801 | 187.381950 | 94.386459 | **60.727460** | 94.007626 |

Table 2 compared the effects of several algorithms with varying input noise levels. When the noise intensity was 0.6 dB, the traditional bat optimization algorithm had an SNR of 13.3%, 17.1%, and 5.2%, greater than both the two enumeration methods and the particle swarm optimization algorithm. The improved bat optimization algorithm had an SNR of 11.3%, greater than the traditional bat optimization algorithm. At 0.8 dB noise intensity, the conventional bat optimization algorithm improved the SNR by 23.3%, 20.7%, and 10.3%, respectively, when compared to the two enumeration methods and particle swarm optimization algorithm. The improved bat optimization algorithm increased the SNR by 8.7% when compared to the conventional bat optimization algorithm. At 1 dB noise intensity, the SNR of the traditional bat optimization algorithm was 26.1%, 25.1%, and 15.1%, higher than that of the two enumeration methods and the particle swarm optimization algorithm, respectively, whereas the improved bat optimization algorithm had an SNR of 10.9%, which was higher than the traditional bat optimization algorithm. Table 3 compared the calculation time of different algorithms. It could be seen from the data in the table that the calculation time of the same algorithm was almost the same under different noise intensities. The code calculation time of the enumeration method was significantly higher than that of other algorithms. The calculation time of the traditional bat algorithm was the best. The computation time of particle swarm optimization was almost the same as that of the improved bat algorithm.

Combine the simulation results in Tables 2 and 3. It could be seen from the data in the table that the SNR obtained by the enumeration method is obviously worse than other algorithms, and the code execution efficiency was the lowest and the running time was the longest. The SNR of the traditional bat algorithm was better than that of particle swarm optimization, and the execution efficiency of the code was obviously improved compared with that of particle swarm optimization. The optimization ability of the improved bat algorithm proposed in this paper was obviously optimal compared with other algorithms, but the running efficiency of the code was almost the same as that of the particle swarm optimization algorithm, which was lower than that of the traditional bat algorithm. In general, the bat algorithm had the advantages of the simple model, fewer parameters, and fast convergence compared with other algorithms.

## 5. Engineering Applications

As a critical piece of equipment for fully mechanized coal mining working faces, the shearer performs the primary function of mining and falling coal. When the shearer is at work, the sound signal generated by the cutting drum contains a wealth of useful information that may represent the current cutting state. However, the working environment at the fully mechanized coal mining working face was poor, and background noise was abundant, resulting in a low SNR for the coal and rock cutting sound signal in the original sound signal collected. This paper analyzed the generation mechanism and propagation process of the sound signal of the coal-rock cutting of the shearer. At the same time, the acoustic signal source and the coupling relationship between the acoustic sources were studied. A time–frequency analysis was made on the sound signals collected in different coal and rock cutting modes and different traction speeds. The influence of coal cutting mode and traction speed on the sound signal was explored. Figure 9a illustrates that the project team constructed a coal-rock cutting experiment platform for a full-size shearer. We collected and analyzed the sound signal generated during coal and rock cutting. To demonstrate the

algorithm's application in practical engineering, the improved bistable stochastic resonance algorithm was used to enhance the sound signal of coal and rock cutting in the original mixed sound signal.


(**a**) (**b**)

**Figure 9.** (**a**) Equipment site layout; (**b**) Sensor installation diagram.

As illustrated in Figure 9b, a sound sensor was mounted on the shearer's side rocker arm facing the sample cutting. The installed sound sensor is a capacitive external bias type with a large diaphragm side acoustic input capable of omnidirectional pointing. The sound sensor transmitted the sound signal collected from the front end to the signal processing device via the MIC-IN interface to accomplish signal preprocessing and adaptive enhancement.

The working speed of the shearer cutting drum was set to 20 r/min in this experiment, resulting in a frequency of 0.33 Hz for the coal-rock cutting sound signal. The sampling frequency *Fs* of the sound sensor was set as 44.1 khz, the sampling time was set as 0.5 s, the signal compression ratio was set as $M$ = 100, and the sampling frequency *fs* after compression was 441 Hz, and the time step and the sampling step were 0.002 s. The noise intensity of additive white Gaussian noise added to the engineering signal was $a^2/(8 \times b)$, with a mean value of 0 and a variance of 1. Figure 10 depicts the time-frequency curve of the signal collected on-site.

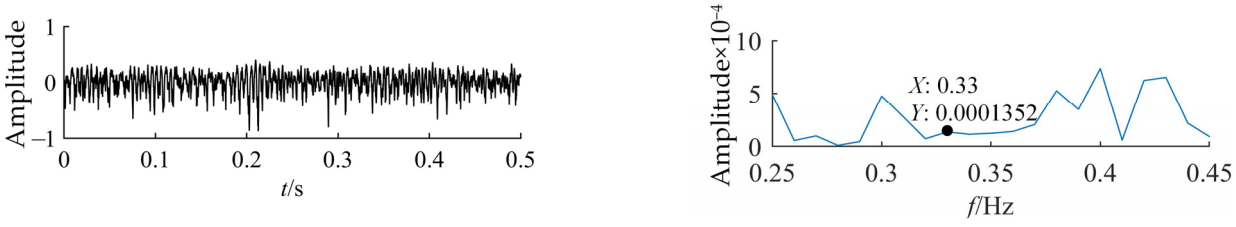


(**a**) (**b**)

**Figure 10.** (**a**) Original sound signal time–domain waveform; (**b**) Original sound signal spectrum.

As illustrated in Figure 10, when the coal-rock cutting sound signal frequency was 0.33 Hz, the corresponding amplitude was 0.0001352 dB, and the corresponding SNR was −22.2339 dB. The coal-rock cutting sound signal occupied a relatively low proportion in the mixed-signal, which was not conducive to the realization of subsequent coal and rock recognition and intelligent control of the Shearer.

The intelligent optimization of two system parameters in the bistable system, a = 0.0186 and b = 0.1025, was carried out using the improved bat optimization algorithm proposed in this paper. The system parameters determined were then substituted into the bistable stochastic resonance model. The mixed sound signals collected were processed, and the resulting time–frequency diagram is shown in Figure 11. As illustrated in Figure 11, the amplitude of the coal-rock cutting sound signal at 0.33 Hz was 34.19 dB, and the corresponding SNR was 20.2198 dB. The comparison demonstrates a 42.4537 dB increase in SNR after the shearer's coal-rock cutting sound signal is processed using the algorithm proposed in this

paper. The energy proportion of the coal-rock cutting sound signal in the whole mixed signal was greatly increased.


**Figure 11.** (**a**) Stochastic resonance model output sound signal time–domain waveform; (**b**) The frequency spectrum of the stochastic resonance model output sound signal.

Finally, this paper compared the enumeration method, the traditional bat optimization algorithm, particle swarm optimization algorithm and the improved bat optimization algorithm in engineering examples. Each algorithm parameter was set in accordance with the simulation data, as shown in Table 4.

**Table 4.** Output comparison with different algorithms.

| Original Signal SNR/dB | Evaluation Indicators/dB | Fixed Parameter *a* | Fixed Parameter *b* | Particle Swarm Optimization | Traditional Bat Algorithm | Improved Bat Algorithm |
|---|---|---|---|---|---|---|
| −22.2339 | SNR | 7.8292 | 9.8674 | 10.8374 | 16.7487 | **20.2198** |

As shown in the table, the bistable stochastic resonance model significantly enhanced the sound signal of coal and rock cutting by the shearer. The model based on the traditional bat optimization algorithm outperformed the enumeration method and particle swarm optimization algorithm, with an increase in SNR of over 5.9113 dB. The signal enhancement algorithm based on the improved bat optimization algorithm was found to be the most effective, and the SNR was increased by 20.7% when compared to the traditional bat algorithm. Compared with the existing algorithms, the IBA-BSR model proposed in this paper has significantly improved convergence, relatively simple structure, and greatly enhanced code efficiency.

## 6. Conclusions and Future Work

This paper combined an improved bat optimization algorithm with a bistable stochastic resonance model to enhance the adaptive signal. It has the potential to significantly increase the ratio of weak target signals in mixed sound signals. We introduce chaotic cubic mapping theory to improve the bat algorithm's global search capability. Finally, the proposed method was applied to simulations and coal-rock cutting sound signals, demonstrating the proposed algorithm's feasibility and superiority. The following are the major conclusions:

(1) Among the simulated signals, the stochastic resonance model based on the improved bat optimization algorithm had the greatest enhancement effect. The improvement was 26.1% and 8.7%, respectively, compared to the enumeration method and traditional bat optimization algorithm.

(2) By comparison, the stochastic resonance model developed using the improved bat optimization algorithm had the greatest effect on the shearer's coal-rock cutting sound signal. The improvement over the enumeration method and the traditional bat optimization algorithm was more than 100.5% and 20.7%, respectively.

(3) The results of simulation and engineering verification showed that the improved bat algorithm proposed in this paper has significantly improved its optimization ability. The execution efficiency of the code was not worse than other algorithms, but it was

slightly worse than the traditional bat algorithm. The algorithm in this paper has a certain effect on increasing the sound signal of coal-rock cutting of shearer, but it is not known how the effect is in other engineering signals. The next step is to study how to improve the operation efficiency of the code and applied it to other kinds of engineering signal processing to further improve the robustness of the algorithm.

**Author Contributions:** J.X. (Jing Xu) and J.X. (Jie Xu) contributed the new method; J.X. (Jie Xu), C.R., Y.L., and N.S. designed the simulations and experiments; J.X. (Jie Xu) and C.R. performed the experiments; J.X. (Jie Xu) wrote the paper. All authors have read and agreed to the published version of the manuscript.

**Funding:** This research was funded by the National Natural Science Foundation of China (No. 51905229), Natural Science Foundation of Jiangsu Province (No. BK20190968), China Postdoctoral Science Foundation (No. 2019M661975), Natural Science Foundation for Colleges and Universities of Jiangsu Province (No. 19KJB460015) and Marine Equipment and Technology Institute of Jiangsu University of Science and Technology (HZ20220001). And the APC was funded by Marine Equipment and Technology Institute of Jiangsu University of Science and Technology (HZ20220001).

**Institutional Review Board Statement:** Not applicable.

**Informed Consent Statement:** Not applicable.

**Data Availability Statement:** Not applicable.

**Acknowledgments:** The author thanks the National Energy Mining Equipment Research Experimental Center of China Coal Zhangjiakou Coal Mining Machinery Co., Ltd. and all the staff for their experimental support.

**Conflicts of Interest:** The authors declare no conflict of interest.

## References

1. Xie, Y.X.; Yan, Y.J.; Li, G.F.; Li, X. Scintillation detector fault diagnosis based on wavelet packet analysis and multi-classification support vector machine. *J. Instrum.* **2020**, *15*, T03001. [CrossRef]
2. Shi, Z.; He, S.L.; Chen, J.L.; Zi, Y.Y. A Dual-Guided Adaptive Decomposition Method of Fault Information and Fault Sensitivity for Multi-Component Fault Diagnosis Under Varying Speeds. *IEEE Trans Instrum Meas* **2022**, *71*, 15. [CrossRef]
3. Sun, Y.K.; Cao, Y.; Xie, G.; Wen, T. Sound Based Fault Diagnosis for RPMs Based on Multi-Scale Fractional Permutation Entropy and Two-Scale Algorithm. *IEEE Trans. Veh. Technol.* **2021**, *70*, 11184–11192. [CrossRef]
4. Qiao, Z.J.; Lei, Y.G.; Li, N.P. Applications of stochastic resonance to machinery fault detection: A review and tutorial. *Mech. Syst. Signal Processing* **2019**, *122*, 502–536. [CrossRef]
5. Yin, J.T.; Tang, J.; Liu, L.; Liu, X.B.; Peng, Z.H.; Li, H. Application of parameter synchronous optimization stochastic resonance in early weak fault diagnosis of traction drive system. *J. Vib. Shock.* **2021**, *40*, 234–240+278.
6. Jiao, S.B.; Gao, R.; Zhang, D.X.; Wang, C. A novel method for UWB weak signal detection based on stochastic resonance and wavelet transform. *Chin. J. Phys.* **2022**, *76*, 79–93. [CrossRef]
7. Benzi, R.; Parisi, G.; Sutera, A.; Vulpiani, A. Stochastic resonance in climatic change. *Tellus* **1982**, *34*, 10–16. [CrossRef]
8. Zhang, G.; Li, H.W. Hybrid tri-stable stochastic resonance system used for fault signal detection. *J. Vib. Shock.* **2019**, *38*, 9–17.
9. Lu, S.L.; He, Q.B.; Wang, J. A review of stochastic resonance in rotating machine fault detection. *Mech. Syst. Signal Processing* **2019**, *116*, 230–260. [CrossRef]
10. Zeng, X.; Lu, X.; Liu, Z.; Jin, Y. An adaptive fractional stochastic resonance method based on weighted correctional signal-to-noise ratio and its application in fault feature enhancement of wind turbine. *ISA Trans.* **2022**, *120*, 18–32. [CrossRef]
11. Liu, J.J.; Leng, Y.G.; Zang, Y.Y.; Fan, S.B. Stochastic resonance with adjustable potential function characteristic parameters and its application in EMU bearing fault detection. *J. Vib. Shock.* **2019**, *38*, 26–33+41.
12. Shi, H.T.; Li, Y.Y.; Zhou, P.; Tong, S.H.; Guo, L.; Li, B.C. Weak Fault Detection for Rolling Bearings in Varying Working Conditions through the Second-Order Stochastic Resonance Method with Barrier Height Optimization. *Shock. Vib.* **2021**, *2021*, 5539912. [CrossRef]
13. Cui, H.J.; Guan, Y.; Chen, H.Y.; Deng, W. A Novel Advancing Signal Processing Method Based on Coupled Multi-Stable Stochastic Resonance for Fault Detection. *Appl. Sci.* **2021**, *11*, 5385. [CrossRef]
14. Liu, J.J.; Leng, Y.G.; Lai, Z.H.; Fan, S.B. Multi-Frequency Signal Detection Based on Frequency Exchange and Re-Scaling Stochastic Resonance and Its Application to Weak Fault Diagnosis. *Sensors* **2018**, *18*, 1325. [CrossRef]
15. Huang, Q.; Liu, J.; Li, H.W. A modified adaptive Stochastic resonance for detecting faint signal in sensors. *Sensors* **2007**, *7*, 157–165. [CrossRef]

16. Wang, S.; Niu, P.J.; Qiao, Z.J.; Guo, Y.F.; Wang, F.Z.; Xu, C.H.; Han, S.Z.; Wang, Y. Maximum cross-correlated kurtosis-based unsaturated stochastic resonance and its application to bearing fault diagnosis. *Chin. J. Phys.* **2021**, *72*, 425–435. [CrossRef]
17. Kang, Y.Q.; Liu, J. Multi-Parameters Adaptive Stochastic Resonance of Genetic Algorithm for Low Concentration Gas Detection. *J. Sens. Technol.* **2019**, *32*, 332–338.
18. Shi, P.M.; Li, M.D.; Zhang, W.Y.; Han, D.Y. Weak signal enhancement for machinery fault diagnosis based on a novel adaptive multi-parameter unsaturated stochastic resonance. *Appl. Acoust.* **2022**, *189*, 108609. [CrossRef]
19. Wang, H.; Chen, J.H.; Zhou, Y.W.; Ni, G.X. Early fault diagnosis of rolling bearing based on noise-assisted signal feature enhancement and stochastic resonance for intelligent manufacturing. *Int. J. Adv. Manuf. Technol.* **2020**, *107*, 1017–1023. [CrossRef]
20. Yang, X.S. A New Metaheuristic Bat-Inspired Algorithm. In *International Workshop on Nature Inspired Cooperative Strategies for Optimization*; Springer: Berlin/Heidelberg, Germany, 2010; Volume 284, pp. 65–74.
21. Agarwal, T.; Kumar, V. A Systematic Review on Bat Algorithm: Theoretical Foundation, Variants, and Applications. *Arch. Comput. Method Eng.* **2021**, 1–30. [CrossRef]
22. Al-Dyani, W.Z.; Ahmad, F.K.; Kamaruddin, S.S. Improvements of bat algorithm for optimal feature selection: A systematic literature review. *Intell. Data Anal.* **2022**, *26*, 5–31. [CrossRef]
23. Mujeeb, S.M.; Sam, R.P.; Madhavi, K. Adaptive Exponential Bat algorithm and deep learning for big data classification. *Sādhanā* **2021**, *46*, 15. [CrossRef]
24. Yue, X.F.; Zhang, H.B. Modified hybrid bat algorithm with genetic crossover operation and smart inertia weight for multilevel image segmentation. *Appl. Soft Comput.* **2020**, *90*, 106157. [CrossRef]
25. Naveen, P.; Sivakumar, P. Adaptive morphological and bilateral filtering with ensemble convolutional neural network for pose-invariant face recognition. *J. Ambient. Intell. Humaniz. Comput.* **2021**, *12*, 10023–10033. [CrossRef]
26. Bangyal, W.H.; Ahmed, J.; Rauf, H.T. A modified bat algorithm with torus walk for solving global optimisation problems. *Int. J. Bio-Inspired Comput.* **2020**, *15*, 1–13. [CrossRef]
27. Shirjini, M.F.; Nikanjam, A.; Shoorehdeli, M.A. Stability analysis of the particle dynamics in bat algorithm: Standard and modified versions. *Eng. Comput.* **2021**, *37*, 2865–2876. [CrossRef]
28. Chen, Z.M.; Tian, M.C.; Wu, P.L.; Bo, Y.M.; Gu, F.F.; Yue, C. Intelligent particle filter based on bat algorithm. *Acta Phys. Sin.* **2017**, *66*, 10. [CrossRef]
29. Yang, Q.D.; Dong, N.; Zhang, J. An enhanced adaptive bat algorithm for microgrid energy scheduling. *Energy* **2021**, *232*, 121014. [CrossRef]
30. Yuan, X.; Yuan, X.W.; Wang, X.H. Path Planning for Mobile Robot Based on Improved Bat Algorithm. *Sensors* **2021**, *21*, 4389. [CrossRef]
31. Tang, H.W.; Sun, W.; Yu, H.S.; Lin, A.; Xue, M. A multirobot target searching method based on bat algorithm in unknown environments. *Expert Syst. Appl.* **2020**, *141*, 112945. [CrossRef]
32. Eskandari, S.; Javidi, M.M. A novel hybrid bat algorithm with a fast clustering-based hybridization. *Evol. Intell.* **2020**, *13*, 427–442. [CrossRef]
33. Zheng, J.G.; Wang, Y.L. A Hybrid Multi-Objective Bat Algorithm for Solving Cloud Computing Resource Scheduling Problems. *Sustainability* **2021**, *13*, 7933. [CrossRef]
34. Mouwafi, M.T.; Abou El-Ela, A.A.; El-Sehiemy, R.A.; Al-Zahar, W.K. Techno-economic based static and dynamic transmission network expansion planning using improved binary bat algorithm. *Alex. Eng. J.* **2022**, *61*, 1383–1401. [CrossRef]
35. He, L.F.; Zhou, X.C.; Zhang, G.; Zhang, T.Q. Stochastic resonance characteristic analysis of the new potential function under Levy noise and bearing fault detection. *J. Vib. Shock.* **2019**, *38*, 53–62. [CrossRef]
36. Leng, Y.G.; Wang, T.Y. Numerical research of twice sampling stochastic resonance for the detection of a weak signal submerged in a heavy Noise. *Acta Phys. Sin.* **2003**, *52*, 2432–2437. [CrossRef]
37. Wang, L.H.; Zhao, X.p.; Zhou, Z.X.; Wu, J.X. Rolling bearings weak fault diagnosis based on adaptive genetic stochastic resonance. *Mod. Electron. Tech.* **2019**, *42*, 40–44.
38. Bezdan, T.; Zivkovic, M.; Bacanin, N.; Strumberger, I.; Tuba, E.; Tuba, M. Multi-objective task scheduling in cloud computing environment by hybridized bat algorithm. *J. Intell. Fuzzy Syst.* **2022**, *42*, 411–423. [CrossRef]
39. Li, J.; Feng, J.J.; Wu, W.J.; Liu, Y.S. Fault diagnosis of power transformer based on improved firefly algorithm and multi-classification support vector machine. *Electr. Meas. Instrum.* **2022**, *59*, 131–135.
40. Wang, C.F.; Di, Y.; Tang, J.Y.; Shuai, J.; Zhang, Y.C.; Lu, Q. The Dynamic Analysis of a Novel Reconfigurable Cubic Chaotic Map and Its Application in Finite Field. *Symmetry* **2021**, *13*, 1420. [CrossRef]
41. Wang, Z.J.; Zhou, J.; Du, W.H.; Lei, Y.G.; Wang, J.Y. Bearing fault diagnosis method based on adaptive maximum cyclostationarity blind deconvolution. *Mech. Syst. Signal Processing* **2022**, *162*, 108018. [CrossRef]